Development 139, 4083-4093 (2012) doi:10.1242/dev.083170

Molecular anatomy of tunicate senescence: reversible function of mitochondrial and nuclear genes associated with budding cycles

Kaz Kawamura[1,*], Seigo Kitamura[1], Satoko Sekida[2], Masayuki Tsuda[3] and Takeshi Sunanaga[1]

SUMMARY

Zooids of the asexual strain of *Polyandrocarpa misakiensis* have a lifespan of 4-5 months; before dying, they produce many buds, enabling continuation of the strain. This study was designed to investigate the nature of gene inactivation and reactivation during this continuous process of senescence and budding. During senescence, the zooidal epidermis showed acid β-galactosidase activity, lost proliferating cell nuclear antigen immunoreactivity and became ultrastructurally worn, indicating that the epidermis is a major tissue affected by the ageing process. Semi-quantitative PCR analysis showed that the genes encoding mitochondrial respiratory chains (MRCs) engaged in decreased transcriptional activity in senescent adults compared with younger adults. The results of in situ hybridization showed that the epidermis dramatically attenuates MRC expression during ageing but restores gene activity when budding commences. During budding and ageing, the nuclear gene *Eed* (a polycomb group component) was activated and inactivated in a pattern similar to that observed in MRCs. In buds, RNA interference (RNAi) of *Eed* attenuated *Eed* transcripts but did not affect the gene expression of pre-activated MRCs. A tunicate humoral factor, TC14-3, could induce *Eed*, accompanying the reactivation of MRC in adult zooids. When RNAi of *Eed* and *Eed* induction were performed simultaneously, zooidal cells and tissues failed to engage in MRC reactivation, indicating the involvement of *Eed* in MRC activation. Results of this study provide evidence that the mitochondrial gene activities of *Polyandrocarpa* can be reversed during senescence and budding, suggesting that they are regulated by nuclear polycomb group genes.

KEY WORDS: Budding, Eed, Mitochondria, Polycomb group, Senescence, Tunicate, *P. misakiensis*

INTRODUCTION

All eukaryotes inevitably undergo *senescence*, which is defined as the time-related deterioration of physiological functions necessary for survival and fertility (Gilbert, 2000; Kirkwood, 2005). Functional deterioration related to senescence can occur at various biological levels. At the tissue level, senescence results in deterioration of homeostatic tissue maintenance (Beerman et al., 2010) and regeneration (Timchenko, 2009). At the cellular level, senescence results in decreased cell proliferation in response to mitogen exposure, injury and other stresses (Iakova et al., 2003). In mammals, senescence-associated β-galactosidase (SA-Gal) is a reliable marker of ageing-related cell growth arrest (Itahana et al., 2007). At the organelle level, senescence accompanies the decrease in mitochondrial respiratory chain (MRC) activity (Byrne et al., 1991). It has been confirmed that one of the main causes of such functional deterioration in mitochondria is the time-related accumulation of DNA damage (Hebert et al., 2010).

Polycomb group (PcG) proteins are multimeric and multifunctional proteins involved in histone modification, a process that leads to genome-wide gene repression (Kuzmichev et al., 2005) and plays a central role in the maintenance of embryonic stem cells (Rajasekhar and Begemann, 2007) and hematopoietic stem cells (Konuma et al., 2010). The primary PcG targets have been considered to be Hox genes; this has now extended to homeodomain-containing and other types of transcriptional regulators (Boyer et al., 2006). In the epidermis (keratinocytes), PcG proteins regulate cell growth, differentiation and senescence (Eckert et al., 2011). In a recent study, we found that TC14-3, a tunicate cytostatic factor, exerts cell growth-inhibitory activity via the gene *embryonic ectoderm development* (*Eed*), a PcG component (Kawamura et al., 2012).

Polyandrocarpa misakiensis belongs to the family *Styelidae* (*Ascidiacea*, *Pleurogona*). However, unlike *Styela* and its other solitary relatives, *P. misakiensis* can propagate by budding (Fig. 1A, 1) (Kawamura et al., 2008a). Buds arise as a double-walled vesicle that protrudes from the parental epidermis and atrial epithelium (Fig. 1A, 2). Differentiated and undifferentiated coelomic mesenchymal cells are located between these outer and inner epithelia (Kawamura and Sunanaga, 2010). Morphogenesis occurs mainly in the inner multipotent epithelium after the buds are detached from the parent (Fig. 1A, 3) (Kawamura and Nakauchi, 1986; Kawamura and Fujiwara, 1994). In ~1 week, these buds become juvenile zooids (Fig. 1A, 4). Approximately 1 month later, the zooids begin to undergo their own budding (Fig. 1A, 1), producing a maximum of 30-40 buds (Oda and Watanabe, 1986) 4-5 months before dying by autolysis (Fig. 1B). The newly formed zooids produced by this process live for an additional 4-5 months before dying themselves. By ensuring the continuation of this process, we have been able to maintain asexual *Polyandrocarpa* strains in Japanese marine stations since 1970 (Fig. 1B) (Kawamura, 1984), when the animals were first collected along the coast of Sagami Bay (Watanabe and Tokioka, 1972). It is interesting to ask how zooidal senescence proceeds over the 4- to 5-month lifespan and how and to what extent senescence events can be reset at each budding event.

[1]Laboratory of Cellular and Molecular Biotechnology, Faculty of Science, Kochi University, Kochi 780-8520, Japan. [2]Laboratory of Cell Biology, Graduate School of Kuroshio Science, Kochi University, Kochi 780-8520, Japan. [3]Division of Animal Reservation, Advanced Research Center, Kochi University, Kochi 783-8505, Japan.

*Author for correspondence (kazuk@kochi-u.ac.jp)

Accepted 3 August 2012

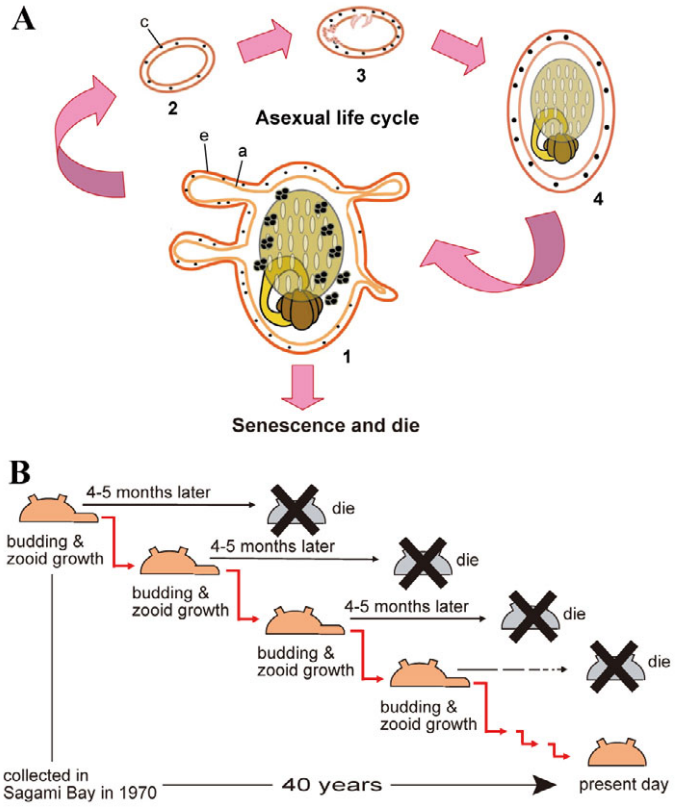

Fig. 1. Asexual life cycle and zooidal senescence of *P. misakiensis*. (**A**) (1) A zooid can form, at most, 30-40 buds anywhere around the basal margin of zooid. (2) Bud consists of outer and inner epithelia and coelomic cells locate between the two epithelia. (3) Bud morphogenesis begins mainly in the inner, atrial epithelium after buds are detached from the parent zooid. (4) In about a week, buds become juvenile zooids. Approximately 1 month later, they begin to form their own buds. a, atrial epithelium; c, coelomic cell; e, epidermis. (**B**) During 4-5 months of asexual life, budding activity gradually decreases and senescent zooids finally die by autolysis. Before dying, zooids give off buds, and the newly formed zooids live for an additional 4-5 months. Thus, we have kept *Polyandrocarpa* asexual strains for more than 40 years in Japanese marine stations.

This study aimed to fulfil four primary goals. The first goal was to determine whether the epidermis is one of the major tissues affected by the ageing process. In doing so, we examined the activity of acid β-galactosidase, referred to as SA-Gal in mammals (Itahana et al., 2007), the nature of cell proliferation and the ultrastructural cell aspects from budding to zooid senescence in *P. misakiensis*. The second goal was to elucidate the gene activity of MRCs, such as NADH dehydrogenase subunit 1 (complex I) and cytochrome *c* oxidase subunit 1 (complex IV), to demonstrate that the transcriptional activity of these genes in the epidermis declines conspicuously during senescence but can be restored during budding. The third goal was to identify nuclear genes that change during budding and senescence with a gene expression pattern similar to that of MRCs. The final goal was to explore whether MRCs could be regulated by upregulating or downregulating *PmEed* gene expression. Results of this study are discussed in the context of novel nuclear and mitochondrial gene interactions in tunicate senescence events.

MATERIALS AND METHODS

Nomenclature

In this study, the term bud refers only to a growing 'bud' still attached to its parent (Fig. 1A, 1; Fig. 2C), a 'juvenile zooid' to a 3- to 4-week-old zooid that has not yet begun to bud (Fig. 1A, 4; Fig. 2B) and a 'senescent zooid' to a zooid aged 18 weeks or older (Fig. 2E). In some experiments, 'developing buds' were additionally used. They separate from the parent (Fig. 1A, 2) and commence morphogenesis (Fig. 1A, 3).

Animals

Asexual strains of *P. misakiensis* (Kawamura, 1984) that had settled in Uranouchi Inlet near the Usa Marine Biological Institute (Kochi University) were cultured on glass slides in culture boxes.

Acid β-galactosidase assay

A modified conventional procedure was used to perform enzyme histochemistry (Choi et al., 2000; Itahana et al., 2007). Animals were fixed in Zamboni's fixative (Zamboni and DeMartino, 1967) for 30 minutes to 1 hour on an ice bath. After thorough washing in chilled phosphate-buffered saline (PBS, pH 7.4), specimens were pre-incubated twice for 10 minutes in 20 mM phosphate buffer (PB, pH 6.0) or 20 mM Na-citrate buffer (pH 6.0). Samples were incubated in a staining solution (3 mM K-ferrocyanide, 3 mM K-ferricyanide, 150 mM NaCl, 1 mM $MgCl_2$, and 0.1% X-gal in the same buffer) overnight at 37°C.

Immunohistochemistry

Animals were fixed in 4% paraformaldehyde in PBS (pH 7.4) for 1 hour in an ice bath, and then serially dehydrated and infiltrated in a plastic resin Technovit 8100 (Heraeus Kulzer, Wehrheim, Germany) for more than 10 hours at 4°C. After hardening, samples were sectioned at 2 μm with glass knives. Sections were pre-treated with 0.01% trypsin in 20 mM Tris Cl (pH 7.6) containing 0.1% $CaCl_2$ for 10 minutes at 30°C, and then with the blocking solution (0.5% skimmed milk in PBS) for 10 minutes at room temperature. Anti-proliferating cell nuclear antigen (anti-PCNA) primary antibody was raised in rabbit using recombinant PCNA from *Botryllus primigenus* as an immunogen and anti-rabbit secondary antibody labelled with horseradish peroxidase (HRP) was purchased from Vector Labs (Burlingame, CA, USA). After antibody staining, sections were washed with PBS containing 0.1% Tween 20 (PBST), and the specimens then coloured with Trueblue dye (KPL, Baltimore, MD, USA). In some sections, the nucleus was counterstained for 10 minutes with 4′,6-diamidino-2-phenylindole (DAPI, 5 μg/ml).

Electron microscopy

Glutaraldehyde (70%) was diluted 30-fold with 0.1 M PB (pH 7.4) containing 1.5% NaCl. The specimens were prefixed with the fixative for 2 hours on ice, and then postfixed with 1% osmium tetroxide in the same buffer for 1 hour on ice. After postfixation, the specimens were rinsed several times with PB containing 1.5% NaCl, dehydrated with a graded acetone series and embedded in Spurr's resin. The resulting resin blocks were sectioned with a diamond knife on an Ultracut UCT ultramicrotome (Leica, Vienna, Austria). Sections were mounted on formvar-coated grids and stained with 1% aqueous uranyl acetate for 1 hour and with lead citrate for 15 minutes in sequence at room temperature. The samples were observed with a Jeol JEM-1400 transmission electron microscope (JEOL, Tokyo, Japan) and photographed using a charge coupled device (CCD) camera.

Reverse-transcription PCR

Poly $(A)^+$ RNA was extracted and purified from buds, juvenile zooids and senescent adult zooids using the biotinyl magnet method according to the manufacturer's protocol (Roche, Mannheim, Land Baden-Württemberg, Germany). Single-stranded DNA complementary to poly $(A)^+$ RNA was synthesized for 1 hour at 42°C by StrataScript reverse transcriptase (Stratagene, Santa Clara, CA, USA). Reverse-transcription PCR (RT-PCR) was performed in two steps: one cycle for sense-strand synthesis (30 seconds at 94°C, 2 minutes at 52°C and 2 minutes at 72°C) and 20-30 cycles of denaturation for 30 seconds at 94°C, annealing for 60 seconds at 52°C and extension for 90 seconds at 72°C. As an internal standard, β-actin cDNA was amplified by PCR.

In situ hybridization

In situ hybridization was performed according to a method previously described (Sunanaga et al., 2007). In brief, after fixation and proteinase K treatment, specimens were hybridized with the digoxigenin (Dig)-labelled antisense ribonucleotide probe for 12-14 hours at 58°C before blocking in 1% skimmed milk in Tris-buffered salt solution containing 0.1% Tween 20 (TBST) for 6 hours on an ice bath. The samples were then treated overnight with anti-Dig monoclonal antibody labelled with alkaline phosphatase (Roche) on ice before being stained with a colour-development solution, dehydrated and embedded in Technovit 8100 resin. Sections were then prepared as described above.

RNA interference

Three different siRNAs were designed from *PmEed* mRNA and purchased from Sigma-Proligo (Tokyo, Japan). Their oligonucletide sequences were as follows: siRNA-1, 5′-AUGCAAACCAAUGUAUCCGUU-3′ and 5′-CGGAUACAUUGGUUUGCAUUU-3′; siRNA-2, 5′-AAAUUAGAAU-AUUUCCAUCUU-3′ and 5′-GAUGGAAAUAUUCUAAUUUGU-3′; siRNA-3, 5′-AACCAUAAGCAUUUCAACCUU-3′ and 5′-GGUUGA-AAUGCUUAUGGUUCU-3′.

The siRNA oligonucleotides were dissolved in filtered seawater. Immediately before use, the same volume of each of the three solutions was mixed at a final concentration of 50 μM. The mixed siRNA was incubated for more than 20 minutes in seawater containing lipofectamine 2000 (10:1; Invitrogen, Carlsbad, CA, USA). Animals were injured with razor blades and treated with the liposome solution for 30 minutes in moist chambers and then returned to the culture box filled with seawater.

RESULTS

Acid β-galactosidase activity in *Polyandrocarpa*

In 1-week-old zooids, no overall acid β-galactosidase activity was detected at pH 6.0, except in the digestive tract (Fig. 2A), where stomach tissue displayed the strongest enzymatic activity (Fig. 2F). This activity in the stomach could be considered the functioning of a digestive enzyme rather than that of acid β-galactosidase. In 4-week-old juvenile zooids immediately prior to budding, the posterior half was observed to have weak enzymatic activity (Fig. 2B). In sections, the pharynx contained many small dotted signals (Fig. 2G), and the epidermis and coelomic mesenchymal cells did not possess as yet any substantial signals (Fig. 2H). In 9-week-old zooids, budding was observed in many areas (Fig. 2C), and although acid β-galactosidase activity appeared to be strong throughout the zooidal body, no staining was observed anywhere in the buds (Fig. 2C, arrowheads). Under neutral pH, β-galactosidase staining entirely disappeared from the zooids, except in the digestive tract (Fig. 2D). In 18-week-old zooids, budding activity was conspicuously reduced (Fig. 2E). The zooid itself was heavily stained, whereas one of small diverticula protruding from the body was not stained (Fig. 2E, arrowhead). In sections, the zooid epidermis had strong enzyme activity (Fig. 2I).

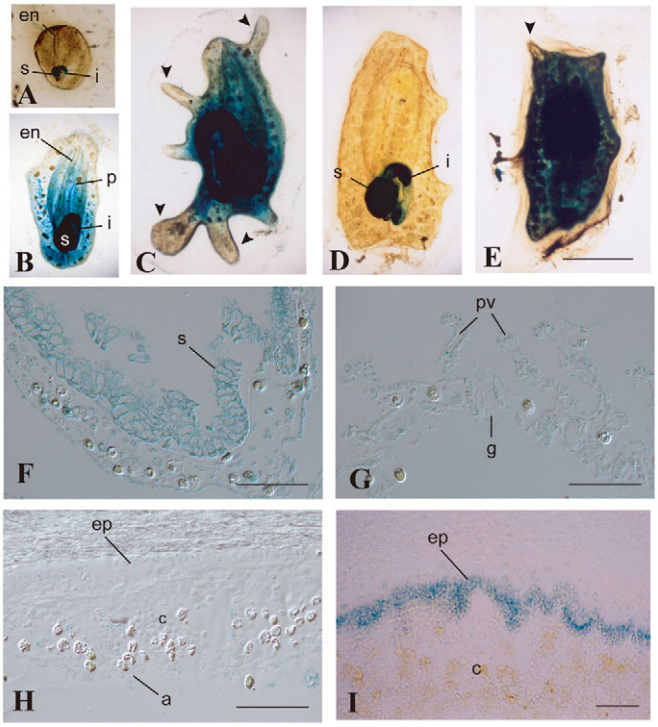

Fig. 2. Enzymatic activity of senescence-associated β-galactosidase in *P. misakiensis*. (A-E) Whole-mount zooids of different ageing stages. Note that adult zooids have stronger signals with age, whereas buds (arrowheads) protruding from the zooids do not show the enzymatic activity. Scale bar: 5 mm. (**A**) Developing bud, 1 week after detached from the parent. (**B**) Juvenile zooid, 4 weeks old. (**C**) Zooid, 9 weeks old. (**D**) Zooid, stained under neutral pH. (**E**) Senescent zooid, 18 weeks old. (F-I) Sections of stained materials. Scale bars: 25 μm. (**F**) Stomach of developing bud. (**G**) Pharynx of juvenile zooid. (**H**) Epidermis and coelomic cells of juvenile zooid. (**I**) Epidermis and coelomic cells of senescent zooid. a, atrial epithelium; c, coelomic cells; en, endostyle; ep, epidermis; g, gill slit; i, intestine; p, pharynx; pv, pharyngeal longitudinal vessel; s, stomach.

PCNA expression during senescence

In buds, strong PCNA signals were detected in the epidermal nuclei (Fig. 3A,B). Signals were also detected in the atrial epithelium (Fig. 3C) and coelomic cells (Fig. 3D), although they were not detected in the morula cells, a type of differentiated blood cell (Fig. 3D, arrowheads). When buds separated from the parent (Fig. 1A, 2), most signals once disappeared from bud tissues (Fig. 3E), and they reappeared at the morphogenetic area of developing buds (Fig. 3F). In juvenile zooids, the epidermal PCNA signals attenuated (Fig. 3G, arrowheads) and became almost undetectable in senescent zooids (Fig. 3I), although proliferative signals were still observable in the atrial epithelial and coelomic cells of juvenile zooids (Fig. 3H) and in a region of coelomic cells of senescent zooids (Fig. 3J). Fig. S1 in the supplementary material shows immunostained pictures merged with DAPI staining. In epidermal cells of growing bud (supplementary material Fig. S1A,B), a total of 21 nuclei out of 24 (87.5%) had strong (black arrowheads) or moderate (grey arrowheads) PCNA signals. In a juvenile zooid (supplementary material Fig. S1C,D), four epidermal nuclei out of 16 were labelled (25%), and in a senescent zooid (supplementary material Fig. S1E,F) only three nuclei out of 41 were moderately labelled (7.3%). Results are statistically summarized in Table 1. In contrast to epidermal cells, the atrial epithelium kept the high score of labelling from buds to juvenile zooids. Coelomic cells also kept relatively high score on average, but the values were variable among sections, depending on the number of co-existing morula cells.

Epidermal morphology during senescence

The bud epidermis was observed to have a cuboidal shape (Fig. 4A,B) and the cytoplasm to contain electron-lucent granules of various sizes (Fig. 4B), which are known to be the pigmented granules that give the epidermis of *Polyandrocarpa* its orange colour (Kawamura and Fujiwara, 1994). Golgi bodies were found to have developed on the apical side facing the tunic (Fig. 4B),

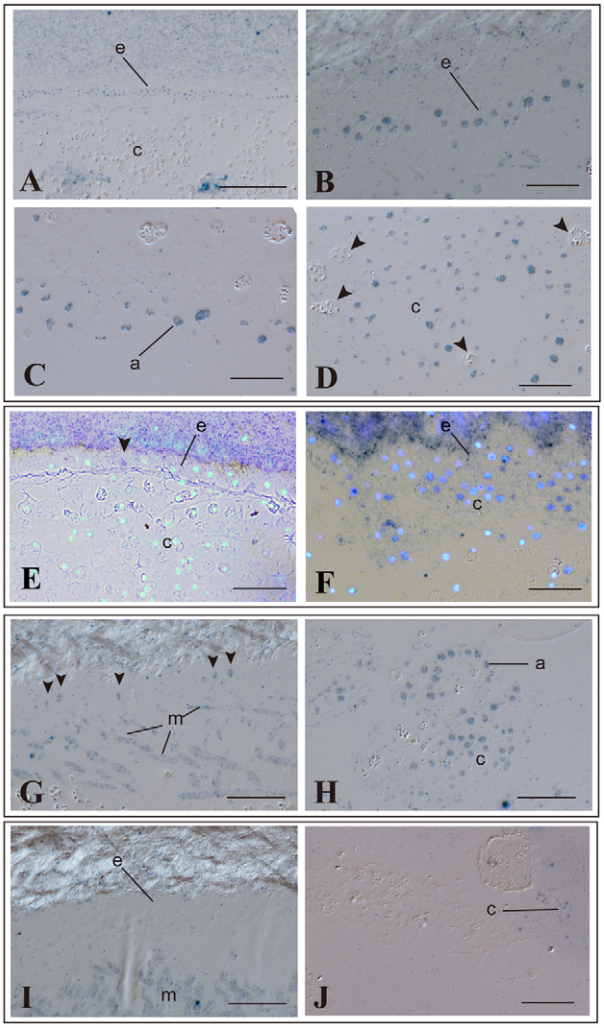

Fig. 3. PCNA expression at different ageing stages, anti-PCNA immunohistochemistry. (A-D) Growing buds. (**A**) Lower magnification. Scale bar: 100 μm. (**B**) Epidermis. Scale bar: 25 μm. (**C**) Atrial epithelium. Scale bar: 25 μm. (**D**) Coelomic cells. Arrowheads show morula cells having no PCNA signals. Scale bar: 25 μm. (E,F) Buds after separation from the parent, merged with DAPI images. (**E**) Epidermis and coelomic cells. A single epidermal cell (arrowhead) had PCNA signal. Scale bar: 25 μm. (**F**) Morphogenetic area of 2-day-old developing bud. Note that PCNA signals reappear. Scale bar: 25 μm. (G,H) Juvenile zooids. (**G**) Epidermis. Several nuclei (arrowheads) were PCNA positive. Nonspecific signals were detected in the cytoplasm of body wall muscle. Scale bar: 25 μm. (**H**) Atrial epithelium and coelomic cells. Many cells were still PCNA positive. Scale bar: 25 μm. (I,J) Senescent zooids. (**I**) Epidermis. No signals were observable. Scale bar: 25 μm. (**J**) Pharynx. Coelomic cells in cluster showed the PCNA signal. Scale bar: 50 μm. a, atrial epithelium; c, coelomic cells; e, epidermis; m, body muscle cell.

whereas most mitochondria were located on the opposing basal side (Fig. 4B). At the cell boundary, the intercellular junction was observed at the apical end (Fig. 4C, arrowhead), and the projections from adjacent cells were tightly interdigitated in the middle (Fig. 4C, star). In juvenile zooids, epidermal cells appeared slender to some extent (Fig. 4D). The cytoplasm was similar to that of the bud epidermis (Fig. 4E). Mitochondria were observed at the basal and middle areas, and the interdigitated junction became loose at the cell boundary (Fig. 4F, star). In senescent zooids, the epidermal cells were observed to have assumed a slender, conical shape (Fig. 4G,H). The adjacent cells lost the indented junction and adhered to one another only by the intercellular junctions, leading to wide spreading of the intercellular space (Fig. 4H). Lysosomes were abundant in the cytoplasm (Fig. 4H). The epidermal mitochondria appeared normal in morphology but the matrix became electron dense in the senescent epidermis, when compared with that of bud and juvenile zooids (Fig. 4I).

When the number of epidermal mitochondria was counted on micrographs of the sections (supplementary material Table S1), it was found to be 8.9±1.4 per 20 μm^2 in growing buds (Fig. 4B,C), 6.9±1.9 per 20 μm^2 in juvenile zooids (Fig. 4E,F) and 6.2±2.0 per 20 μm^2 in senescent adults (Fig. 4H,I).

MRC gene expression during senescence

The cDNA for cytochrome c oxidase subunit 1 (*PmCOX1*, AB591739) was 1526 bp long and it encoded 507 amino acid residues. The cDNA for NADH dehydrogenase subunit 1 (*PmND1*, AB591740) was 915 bp long, encoding 304 amino acid residues. The RT-PCR analyses showed that *PmCOX1* and *PmND1* transcripts were abundant in buds and juvenile zooids but remarkably weak in senescent adults (supplementary material Fig. S2).

Spatiotemporal gene expression of MRCs was examined by in situ hybridization. In growing buds, *PmCOX1* was widely expressed in the epidermis (Fig. 5A,B), coelomic cells and the atrial epithelium (Fig. 5C). Juvenile zooids showed similar but somewhat lower staining of the epidermis, atrial epithelium and coelomic cells (Fig. 5D-F). In senescent zooids, the epidermal signal declined to an undetectable level (Fig. 5G). In the coelomic space, signals attenuated, but in places they remained in cell clusters (Fig. 5H). Among differentiated tissues, *PmCOX1* was weakly expressed in the oesophagus, stomach and intestine (supplementary material Fig. S3A-D). In the gonad, germline precursor cells and oocytes continuously expressed *PmCOX1* (supplementary material Fig. S3E,F).

To determine whether decreased *PmCOX1* signals in the epidermis was due to artefactual infiltration of probes in adult tissues, the expression of *Pmβ-Catenin* was examined in senescent adult zooids as a positive control. The epidermis and coelomic cells emitted clear signals (Fig. 5I).

Fig. S4 in supplementary material shows *PmND1* expression. In buds, the epidermis was stained most strongly and extensively (supplementary material Fig. S4A,B). Coelomic cells and the atrial epithelium were also stained (supplementary material Fig. S4C). In juvenile zooids, epithelial tissues and coelomic cells were stained to an extent similar to that of buds (supplementary material Fig. S4D-F). In senescent adults, signals became very weak in the epidermis, atrial epithelium, coelomic cells, pharynx and endostyle (supplementary material Fig. S4G-K). In the gonad, punctuated strong signals emitted from the oocyte cytoplasm (supplementary material Fig. S4L).

MRC reactivation during budding

Fig. 6A shows whole-mount staining of *PmCOX1* in an adult zooid piece that has two protruding buds. In the bud primordium (Fig. 6A, right open box), the epidermis already has a strong signal, as demarcated by arrowheads from the parent epidermis (Fig. 6B,C). Signals were also evident in coelomic cells (Fig. 6D). In growing buds, the epidermal slope (Fig. 6A, left open box) showed a gradual increase in signal from the adult zooid (with no signal) to the bud (with a strong signal) (Fig. 6E). The bud primordium could also

Table 1. The number of PCNA-expressing nuclei in the epidermis, atrial epithelium and coelomic cells during budding and senescence of *P. misakiensis*

Tissues	*n*	Epidermis	Atrial epithelium	Coelomic cells
Buds	125* (5)‡	84.8±3.2§,¶	74.5±4.4	45.2±15.5
Juvenile zooids	100 (4)	28.1±3.5	75.5±8.2	40.6±15.8
Senescent zooids	100 (4)	7.5±0.5	10.1±5.6	25.6±16.5

*Number of sections examined.
‡Number of animals sectioned.
§Average±s.d.
¶Nuclei expressing PCNA strongly or moderately were counted per 100 cells.

reactivate *PmND1* (Fig. 6F). The boundary of *PmND1* expression (Fig. 6G,H, arrowheads) was consistent with that of *PmCOX1* expression in double fluorescent in situ hybridization (not shown).

PmEed expression during senescence and budding

A cDNA for *Eed* (*PmEed*, AB617630), a *Polyandrocarpa* polycomb group component, was 920 bp long and its deduced amino acid sequence was most similar to that of *Ciona Eed* on the molecular phylogenetic tree (supplementary material Fig. S5). The RT-PCR analyses showed that in senescent adults, the *PmEed* expression was substantially less than that of buds and juvenile zooids (supplementary material Fig. S2). By in situ hybridization of buds, the epidermis, atrial epithelium and coelomic cells extensively expressed *PmEed* (Fig. 7A-C). Signals in the coelomic space mainly emitted from undifferentiated cells with a large nucleus and narrow cytoplasm (Fig. 7B, arrowheads) and from granular cells (Fig. 7B,C, arrows) but not from morula cells (Fig. 7C). The expression was maintained in juvenile zooids (Fig. 7D-G), especially in the coelomic undifferentiated cells (Fig. 7E, broken circle), gonad rudiment (Fig. 7F, arrowhead) and pharyngeal epithelium (Fig. 7G). In senescent adults, however, the signal disappeared from the epidermis and most other tissues, except the gonad (Fig. 7H-J). In the gonad, the germinal vesicle of young oocyte, follicle cells and small coelomic cells were heavily stained (Fig. 7J).

Effect of *PmEed* on mitochondrial gene expression

When buds were treated with siRNA(*PmEed*), *PmEed* signals conspicuously diminished from the buds (Fig. 8A-C) and, inversely, PCNA signals were extended ectopically from morphogenetic, proximal area of bud (31 nuclei out of 38; Fig. 8D,E,E′) toward the non-morphogenetic distal area (12 nuclei out of 26; Fig. 8D,F,F′) through the lateral body wall (Table 2). The results indicated that the RNAi of *PmEed* efficiently acted on buds. By contrast, the siRNA(*PmEed*) treatment was found not to attenuate the gene expression of *PmCOX1* at the proximal and distal areas of bud (Fig. 8G-I), indicating that RNAi has no effect on mitochondrial gene activity that has already been enhanced during budding.

A recent study has suggested that TC14-3, a tunicate cytostatic factor, is able to induce gene expression of both *PmEed* and *PmCOX1* in adult zooids (Kawamura et al., 2012). Similar results were obtained in the present study (supplementary material Fig. S6; Fig. 9A). Further experiments were designed to disclose whether or not siRNA(*PmEed*) is able to cancel TC14-3-induced enhancement of *PmCOX1* gene expression in *Polyandrocarpa* adult zooids. In the negative control, in which zooids were only cut into pieces, both *PmEed* and *PmCOX1* showed faint signals by RT-PCR (Fig. 9A, lane 1). By in situ hybridization, zooid pieces did not exhibit *PmCOX1* signal (Fig. 9B,C). In the positive control,

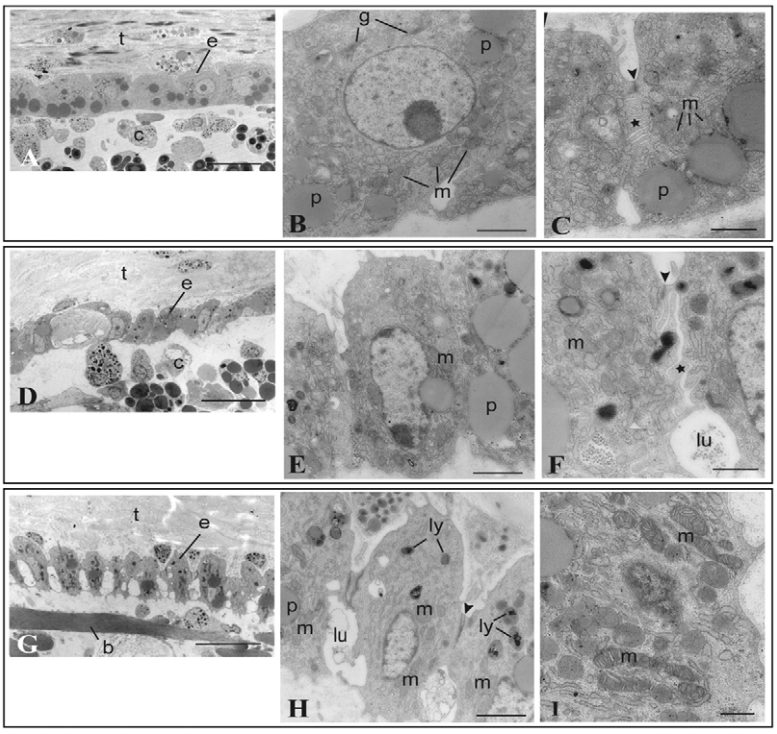

Fig. 4. Epidermal morphology at different ageing stages, electron microscopy. (A-C) Growing buds. (**A**) Lower magnification. Note that each epidermal cell takes cuboidal shape. Scale bar: 10 μm. (**B**) Single epidermal cell. Scale bar: 2 μm. (**C**) Cell boundary. Arrowhead shows the adherens intercellular junction. Star shows the interdigited junction. Scale bar: 1 μm. (D-F) Juvenile zooids. (**D**) Lower magnification. Scale bar: 10 μm. (**E**) Epidermal cells. Scale bar: 2 μm. (**F**) Cell boundary. Arrowhead shows the adherens junction. The interdigited junction (star) becomes less complicated. Scale bar: 1 μm. (G-I) Senescent zooids. (**G**) Lower magnification. Note that each epidermal cell becomes slender. Scale bar: 10 μm. (**H**) Epidermal cells. Between adjacent cells a large lumen instead of interdigitation is found. Scale bar: 2 μm. (**I**) Morphology of mitochondria. Scale bar: 1 μm. b, body muscle cell; c, coelomic cell; e, epidermis; g, golgi body; l, lysosome; lu, lumen; m, mitochondria; p, pigment granule; t, tunic.

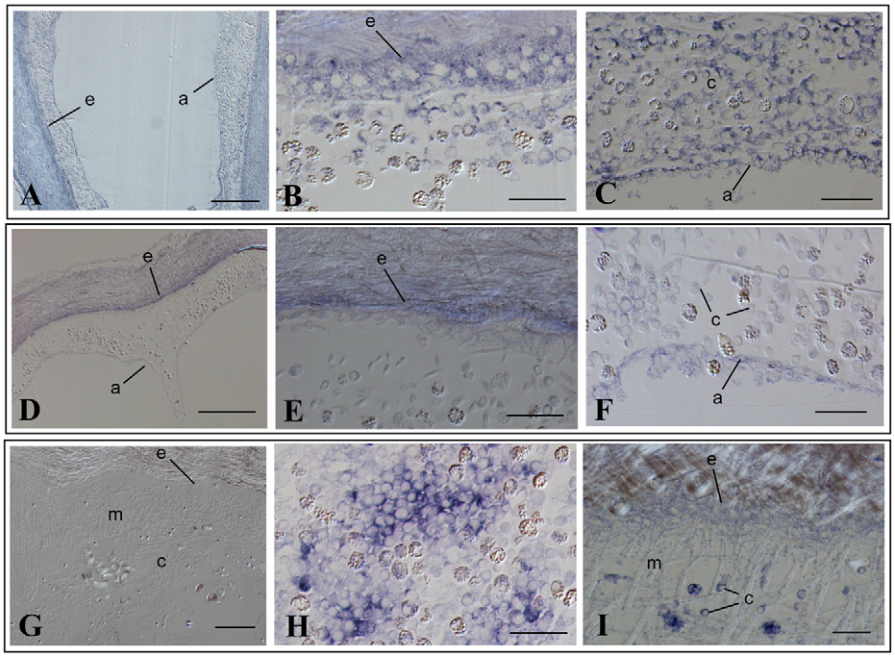

Fig. 5. *PmCOX1* expression at different ageing stages, in situ hybridization. (A-C) Growing buds. (**A**) Frontal section of bud. Scale bar: 200 μm. (**B**) Epidermis and coelomic cells. Scale bar: 20 μm. (**C**) Atrial epithelium and coelomic cells. Scale bar: 20 μm. (D-F) Juvenile zooids. (**D**) Frontal section of the posterior area of zooid. Scale bar: 100 μm. (**E**) Epidermis and coelomic cells. Scale bar: 20 μm. (**F**) Atrial epithelium and coelomic cells. Scale bar: 20 μm. (G-I) Senescent zooids. (**G**) Body wall of zooid. Scale bar: 100 μm. (**H**) *PmCOX1*-positive coelomic cell cluster. Scale bar: 20 μm. (**I**) Positive control, β-catenin staining of zooid. Note that the epidermis has signals. Scale bar: 20 μm. a, atrial epithelium; c, coelomic cell, e, epidermis; m, body muscle cell.

zooid pieces were treated with TC14-3. They expressed both genes of *PmEed* and *PmCOX1* (Fig. 9A, lane 2). The pharynx and coelomic cells strongly expressed *PmCOX1* (Fig. 9D-F), whereas epidermal cells showed moderate signals in some places and no signals in other places on the same section (Fig. 9G,H), which would be because of the low infiltration of TC14-3 within zooid tissues. However, when the TC14-3-treated zooid pieces were further treated with siRNA(*PmEed*), the induction of *PmCOX1* was suppressed to a large extent (Fig. 9A, lane 3). The epidermis and pharynx did not show *PmCOX1* signals (Fig. 9I), and coelomic cells showed very weak signals (Fig. 9J), suggesting that *PmEed* is necessary for TC14-3-mediated mitochondrial gene activation.

DISCUSSION

Impact of ageing on epidermal tissue in *P. misakiensis*

In mammals, acid β-galactosidase, which works efficiently in the lysosome at pH 6.0 (Lee et al., 2006), is a reliable marker of senescent cells (Itahana et al., 2007). In *P. misakiensis*, acid β-galactosidase activity became histochemically stronger with ageing, although, under neutral pH, it disappeared from all tissues with the exception of the digestive tract. Growing buds did not have the enzyme activity, even though the parent zooid exhibited strong signals. It should also be noted that several bud primordia from senescent adult zooids still have the enzyme activity, suggesting that the disappearance of acid β-galactosidase is not a necessary pre-requisite for bud formation. In juvenile zooids, the pharynx had many small dotted signals of probably lysosomal origin. The epidermis of senescent adult zooids emitted the strongest signals from the whole cytoplasm that was ultrastructurally abundant in lysosome, indicating enhanced lysosomal activities in aged epidermis. These results suggest that acid β-galactosidase activity in *Polyandrocarpa* is homologous to that of SA-Gal in mammals.

In many organisms, senescence accompanies cell-growth arrest, which results in defects in tissue repair and regeneration (Iakova et al., 2003; Yang and Fogo, 2010). Previous autoradiographic studies of *P. misakiensis* using [^{3}H]thymidine showed that in growing buds, the labelling index of epidermal cells was 3.7±0.4% (Kawamura et al., 1988), a value considerably higher than that measured in adult zooids. Labelled cells remarkably decreased in number temporarily after bud isolation from the parent. In this study, most cells of the bud epidermis were found to emit PCNA signals. They lost the signals temporarily at the transition period between the bud growth phase and the developmental phase, and they resumed the signals at the morphogenetic area of developing buds, consistent with the results of [^{3}H]thymidine incorporation. By contrast, the epidermis of senescent adults has stopped engaging in extensive PCNA signals, consistent with the previous autoradiographic studies.

In *P. misakiensis*, the epidermis has severely undergone cell morphological changes during senescence. Specifically, adult epidermal cells become lean; the intercellular space has widened by the loss of interdigitated junction; many neighbouring cells remain connected only by the adherens intercellular junction; epidermal cells contain a larger number of lysosomes in the cytoplasm; the number of mitochondria decreases to some extent; and the mitochondrial matrix becomes darker than the translucent matrices in the bud epidermis, suggesting the accumulation of electron-absorbing wastes in the mitochondrial matrix in the senescent epidermis. Most interestingly, the epidermis has attenuated the transcriptional activity of several mitochondrial and nuclear genes during senescence.

These findings indicate that in *P. misakiensis*, the epidermis is one of the major tissues affected by the ageing process. This indication is further highlighted by comparison with two types of *Polyandrocarpa* multipotent cells: hemoblasts, which are undifferentiated cells in the hemocoel (Kawamura and Sunanaga, 2010); and cells of the atrial epithelium, which conducts cell proliferation and transdifferentiation during budding and regeneration (Kaneko et al., 2010; Kawamura and Fujiwara, 1994; Kawamura and Nakauchi, 1986; Kawamura et al., 2008a). These two types of cells do not express SA-Gal, even when the epidermis shows strong enzyme activity. PCNA signals were still observable in the atrial epithelium of the juvenile zooids, and even in a small number of the undifferentiated coelomic cells of senescent adult

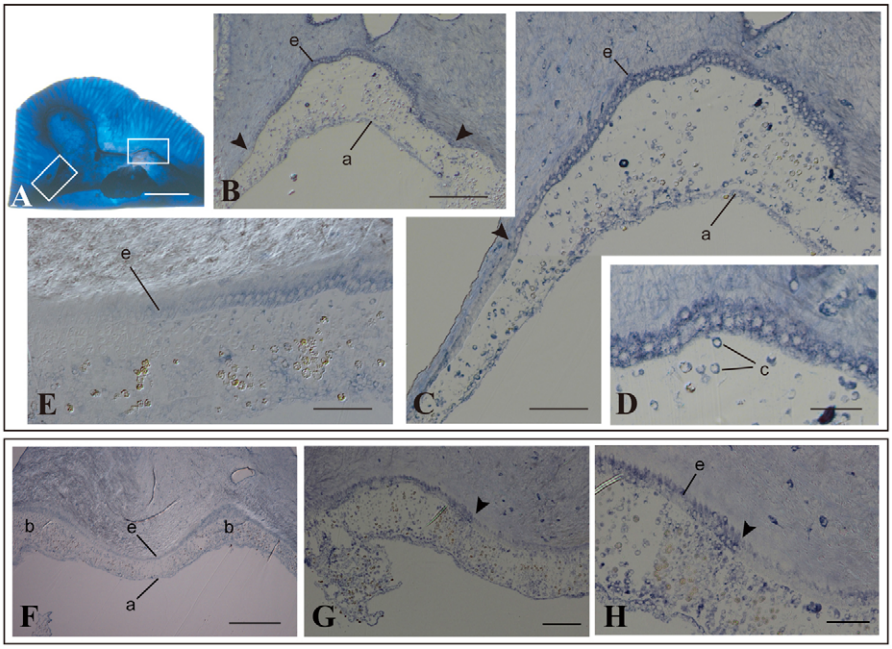

Fig. 6. Reactivation of MRC genes during budding. (A-E) *PmCOX1*. (**A**) A whole-mount of adult zooid with two protruding buds. An open box on the right side shows the bud primordium. A left-sided open box shows the zooid-bud boundary. Scale bar: 1 mm. (**B**) Bud primordium. Arrowheads show the boundaries of the primordium. Scale bar: 100 μm. (**C**) Higher magnification of bud primordium. Scale bar: 50 μm. (**D**) Distal tip of bud epidermis. Scale bar: 20 μm. (**E**) Zooid-bud boundary. Note the gradual increase in *PmCOX1* signals in the foot area of bud. Scale bar: 50 μm. (F-H) *PmND1*. (**F**) Two bud primordia. Scale bar: 0.5 mm. (**G**) Bud primordium. Arrowhead shows the boundary of the primordium. Scale bar: 100 μm. (**H**) Higher magnification of the boundary (arrowhead). Scale bar: 50 μm. a, atrial epithelium; b, bud primordium; c, coelomic cell; e, epidermis.

zooids. Nodules of undifferentiated coelomic cells continued to express mitochondrial genes in the hemocoel of senescent adult zooids.

Reversible function of mitochondrial genes during budding

In senescent adult zooids of *P. misakiensis*, the epidermis was found to have almost entirely ceased the gene expression of both *PmCOX1* and *PmND1*. As previously described, the number of epidermal mitochondria has decreased to some extent during senescence, but it is unlikely that this decrease is the main cause of the conspicuous decrease in MRC gene activity in *Polyandrocarpa*. In this connection, we observed that during senescence of *P. misakiensis*, Cu/Zn-superoxide dismutase (*SOD1*) but not *SOD2* decreased gene activity specifically in the epidermis (K.K., unpublished). To mimic the decrease in *SOD1* gene activity during

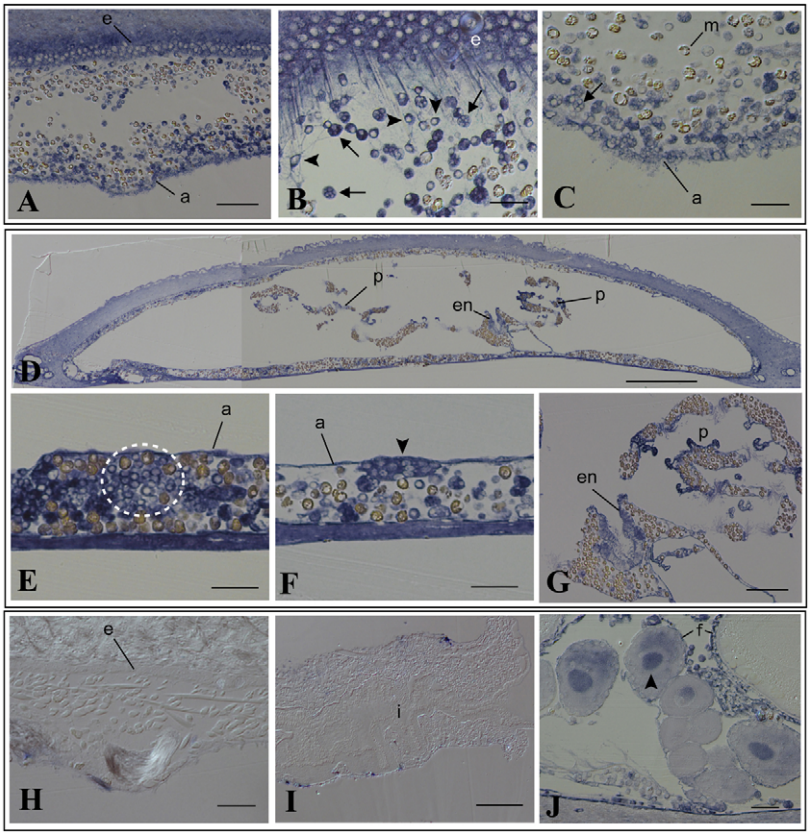

Fig. 7. *PmEed* expression at different ageing stages, in situ hybridization. (A-C) Growing buds. (**A**) Body wall of bud. Scale bar: 50 μm. (**B**) Epidermis and coelomic cells. Arrows and arrowheads show granular cells and undifferentiated cells, respectively. Scale bar: 20 μm. (**C**) Atrial epithelium and coelomic cells. Arrow shows granular cell. Scale bar: 20 μm. (D-G) Juvenile zooids. (**D**) Transverse section. Scale bar: 200 μm. (**E**) Ventral body wall. Broken circle shows an aggregate of undifferentiated cells. Scale bar: 20 μm. (**F**) Ventral body wall. Arrowhead shows a possible gonad rudiment. Scale bar: 20 μm. (**G**) Pharynx and endostyle. Scale bar: 50 μm. (H-J) Senescent adult zooid. (**H**) Dorsal body wall. Scale bar: 20 μm. (**I**) Digestive tract. Scale bar: 100 μm. (**J**) Gonad. Arrowhead shows the germinal vesicle of a young oocyte. Scale bar: 20 μm. a, atrial epithelium; e, epidermis; en, endostyle; f, follicle cell; i, intestine; m, morula cell; p, pharynx.

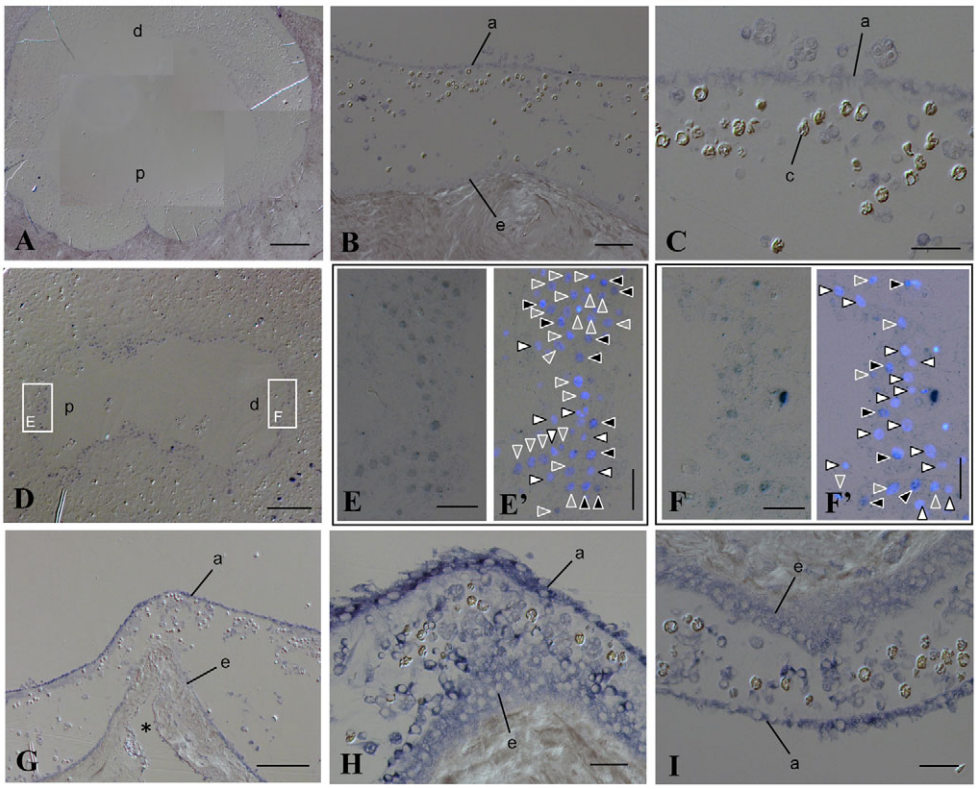

Fig. 8. Effects of siRNA(*PmEed*) on 2-day-old developing buds of *P. misakiensis*. (A-C) *PmEed* in situ hybridization. (**A**) Lower magnification of bud. Scale bar: 200 μm. (**B**) Proximal area of bud. Scale bar: 50 μm. (**C**) Atrial epithelium and coelomic cells. Scale bar: 20 μm. (D-F) PCNA immunohistochemistry. (**D**) Lower magnification of bud. Scale bar: 100 μm. (**E**) Proximal area of bud. Scale bar: 20 μm. (**E′**) Immunostained nuclei merged with DAPI staining. Black and gray arrowheads show nuclei of the atrial epithelium expressing PCNA strongly and moderately, respectively. White arrowheads show PCNA-negative nuclei. Scale bar: 20 μm. (**F**) Distal area of bud. Scale bar: 20 μm. (**F′**) Immunostained nuclei merged with DAPI staining. Black and gray arrowheads show nuclei of the atrial epithelium expressing PCNA strongly and moderately, respectively. White arrowheads show PCNA-negative nuclei. Scale bar: 20 μm. (G-I) *PmCOX1* in situ hybridization. (**G**) Proximal area of bud. Asterisk shows the trace of surgical operation. Scale bar: 100 μm. (**H**) Higher magnification of the proximal area. Scale bar: 20 μm. (**I**) Distal area of bud. Scale bar: 20 μm. a, atrial epithelium; c, coelomic cell; d, distal area of bud; e, epidermis; p, proximal area of bud.

senescence, *Polyandrocarpa* juvenile zooids were treated with siRNA(*PmSOD1*) and the resultant zooids were observed to prematurely attenuate MRC activity (K.K., unpublished). It is, therefore, possible to assume that during normal senescence of *P. misakiensis*, the decrease in *PmSOD1* gene expression should be one of main causes of the downregulation of MRC gene activities.

In human skeletal muscle, it is well known that MRC functions deteriorate with ageing (Boffoli et al., 1994; Byrne et al., 1991; Cooper et al., 1992), depending on the low activities of complexes I (NADH dehydrogenase) and IV (cytochrome oxidase) (Cooper et al., 1992). This decrease in MRC functions may be caused by mutations in mitochondrial genes (Byrne et al., 1991; Hebert et al., 2010). Indeed, cytochrome oxidase has been observed to alter polypeptide patterns during ageing (Boffoli et al., 1994). However, it is unlikely that during senescence of *P. misakiensis*, irreversible deterioration, such as a genetic mutation, has occurred in the epidermal mitochondrial genome, because epidermal MRCs can be activated at every budding. We found that this reactivation has already begun in the bud primordium. The repeatable mitochondrial gene function related to budding (asexual reproduction) is quite a novel finding.

Reversible function of nuclear gene during budding

Recently, we suggested that budding in *P. misakiensis* reinforced the gene activity of *Eed* (Kawamura et al., 2012). In this paper, we present further evidence that *PmEed* is activated in most bud tissues and attenuated in most senescent zooid tissues with an exception of gonads. The tunicate cytostatic factor, TC14-3, is a

Table 2. Effect of siRNA(PmEed) on PCNA expression in 2-day developing buds of *P. misakiensis*

	n	Proximal	Lateral	Distal
Control, siLacZ-treated	100* (4)‡	80.2±5.9§,¶	12.8±2.8	4.1±1.8
Experiment, siPmEed-treated	100 (4)	78.9±4.0	58.8±3.8	55.6±5.1

*Number of sections examined.
‡Number of animals sectioned.
§Average±s.d.
¶Nuclei expressing PCNA strongly or moderately were counted per 100 cells.

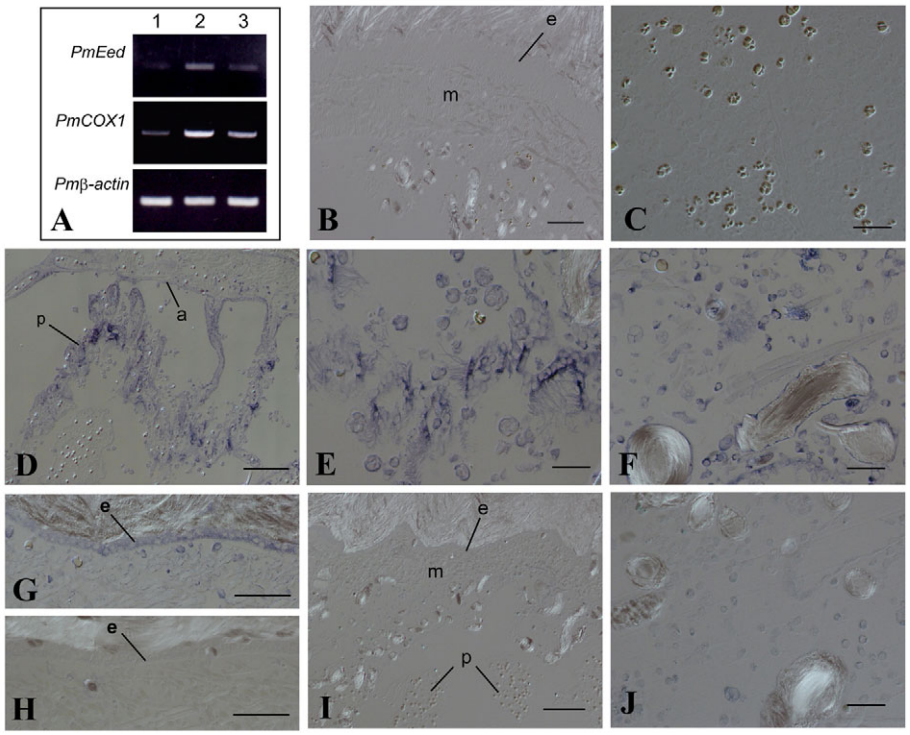

Fig. 9. Effect of siRNA(*PmEed*) on *Polyandrocarpa* zooid pieces treated with TC14-3. (**A**) RT-PCR of *PmEed*, *PmCOX1* and *Pmβ-actin*. Lane 1, negative control untreated with TC14-3 and siRNA(*PmEed*). Lane 2, positive control treated with TC14-3. Lane 3, experiment treated with both TC14-3 and siRNA(*PmEed*). (B-J) *PmCOX1* in situ hybridization. (B,C) Negative control. (**B**) Body wall of zooid. Scale bar: 50 μm. (**C**) Coelomic cells in the hemocoel. Scale bar: 20 μm. (D-H) Positive control. (**D**) Pharynx of zooid. Scale bar: 100 μm. (**E**) Higher magnification of the pharynx. Scale bar: 20 μm. (**F**) Coelomic cells in the hemocoel. Scale bar: 20 μm. (**G**) Epidermis having moderate signals. Scale bar: 40 μm. (**H**) Epidermis having no signals on the same section as G. Scale bar: 40 μm. (I,J) Experiment. (**I**) Body wall and pharynx of zooid. Scale bar: 100 μm. (**J**) Coelomic cells in the hemocoel. Scale bar: 20 μm. a, atrial epithelium; e, epidermis; m, muscle cell; p, pharynx.

budding-specific, humoral polypeptide (Matsumoto et al., 2001). It can induce *PmEed* in vivo and in vitro (Kawamura et al., 2012), which would explain how *PmEed* is reactivated during budding.

In mammals, *Eed* is expressed in undifferentiated embryonic cells and is undetectable in differentiated cells (Kuzmichev et al., 2005). Eed constitutes polycomb repressive complex 2 (PRC2) and stimulates histone methyltransferase activity of PRC2 (Konuma et al., 2010). Likewise, in *P. misakiensis*, the induction of *PmEed* stimulated trimethylation of histone H3 at Lys27 (Kawamura et al., 2012). In general, histone modification by PcG leads to genome-wide gene repression (Kuzmichev et al., 2005), which plays a central role in the maintenance of embryonic stem cells (Rajasekhar and Begemann, 2007) and hematopoietic stem cells (Konuma et al., 2010). In the epidermis (keratinocytes), PcG proteins negatively regulate cell growth and differentiation (Eckert et al., 2011). In *P. misakiensis*, RNAi of *PmEed* has been found to preserve culture cells from the growth-inhibitory effect of TC14-3 (Kawamura et al., 2012) and, as shown in this paper, RNAi of *PmEed* has caused the in vivo ectopic expression of PCNA in developing buds, findings that are consistent with the well-known cell growth-inhibitory effect of PcG.

Involvement of nuclear genes in reversible mitochondrial gene activities

PcG proteins regulate not only cell growth and differentiation but also senescence (Eckert et al., 2011). As already described, tunicate senescence is deeply associated with MRC gene activity. As first suggested by Kawamura et al. (Kawamura et al., 2012) and confirmed in the present study, TC14-3 enhances the gene expression of *PmCOX1* as well as *PmEed*. To determine whether *PmEed* was directly involved in MRC gene regulation, growing buds were treated with siRNA(*PmEed*) and strong *PmCOX1* expression was observed to remain in the epidermis, atrial epitheliu, and coelomic cells, indicating that RNAi of *PmEed* does not affect MRCs that are pre-activated during budding. By contrast, when zooid pieces were treated with both siRNA(*PmEed*) and TC14-3, MRC activation did not occur although it was observed in zooid pieces treated solely with TC14-3. This finding provides the first piece of evidence that Eed, a component of PcG, is involved in the rejuvenation of mitochondria. An intriguing issue is whether TC14-3 can contribute to zooidal longevity in *P. misakiensis*. As most of senescent zooid pieces became dormant instead of completing regeneration in the presence or absence of TC14-3, it is uncertain at present whether TC14-3 can influence the zooidal lifespan.

It is unlikely that Eed and/or PcG directly act on the mitochondrial genome, as the mitochondrial genome does not have histones. In humans, transcription levels of mitochondrial genes are stably maintained by the nuclear transcriptional regulatory factor Tfam (Kelly and Scarpulla, 2004; Scarpulla, 2008). In *P. misakiensis*, a *Tfam*-like gene belonging to the high mobility group genes was highly expressed during budding and this transcription level decreased conspicuously during senescence (K.K., unpublished). This finding suggests that the *PmTfam*-like gene may be related to MRC gene regulation through TC14-3-induced PcG and/or histone methylation. It is probable, therefore, that in *P. misakiensis*, several nuclear genes appear to be involved in reversible MRC functions in association with budding cycles.

Other features of tunicate senescence

As already mentioned, *PmSOD1* is a senescence-dependent nuclear gene. SOD protects cells and tissues from oxidative stress due to reactive oxygen species (ROS), and human SOD1 can extend the normal lifespan of *Drosophila* by up to 40% (Parkes et al., 1998). In *P. misakiensis*, *PmSOD1* expression has been observed to cease in the epidermis, while continuing weakly in other tissues, including the pharynx, endostyle and stomach and, exceptionally, continuing strongly in germ cells (K.K., unpublished). Such strong expression helps protect germ cells from oxidative stress, genetic mutation and cell death due to ROS production (Liu et al., 2000).

Botryllus schlosseri is a colonial tunicate related to *P. misakiensis*. In a colony, adult zooids are taken over by the younger generation every 5-7 days. At this takeover stage, tissues and organs of the adult zooids disintegrate and fragment into apoptotic bodies, followed by the ingestion by coelomic macrophages or intraepithelial phagocytes (Burighel and Schiavinato, 1984; Lauzon et al., 1993; Tiozzo et al., 2006). In *B. primigenus*, most cells and tissues of adult zooids become mitotically quiescent before apoptosis (Kawamura et al., 2008b). In a previous investigation of *B. primigenus*, we detected SA-Gal activity in the apoptotic cell mass of degenerating zooids but not in the epidermis and other tissues of functional adult zooids or younger generations (K.K., unpublished).

In *Botryllus*, aged colonies accumulate pigment cells in the hemocoel until they can grow no further, leading to colonial death in a phenomenon referred to as nonrandom colonial senescence (Lauzon et al., 2000). When we examined SA-Gal activity during non-random colonial senescence in *B. primigenus*, the enzyme activity was observed to increase remarkably in the coelomic space but, unlike *P. misakiensis*, no signals were detected in the epidermis (K.K., unpublished). Taken together, the findings regarding zooidal takeover and colonial senescence in *Botryllus* appear to take cellular features different from zooidal senescence in *Polyandrocarpa*.

Conclusions

Senescence inevitably deteriorates physiological functions necessary for survival and fertility. It accompanies the mitochondrial dysfunction caused by the time-related accumulation of DNA damage. Only germ cells and stem cells are considered as exceptional cells that can escape from such dysfunction. In *P. misakiensis*, senescence events accompany mitochondrial dysfunction similar to other biological systems, but senescence in this species is unique because all ageing events examined are reversible and repeatable during budding, even in epidermal non-stem cells. Several nuclear genes are involved in such reversible senescence events. A candidate nuclear gene is *Eed*, which is a component of PcG. *Eed* can indeed mediate mitochondrial reactivation in senescent adult zooids. In conclusion, our results afford new insights into the function of PcG concerning the resetting or reprogramming of cellular senescence and mitochondrial rejuvenation.

Acknowledgements

We thank Dr Shigeki Fujiwara for valuable suggestions and encouragement throughout the course of study.

Funding

This study was supported in part by the Japan Society for the Promotion of Science grant [21570227] to K.K.

Competing interests statement

The authors declare no competing financial interests.

Supplementary material

Supplementary material available online at
http://dev.biologists.org/lookup/suppl/doi:10.1242/dev.083170/-/DC1

References

Beerman, I., Maloney, W. J., Weissmann, I. L. and Rossi, D. J. (2010). Stem cells and the aging hematopoietic system. *Curr. Opin. Immunol.* **22**, 500-506.

Boffoli, D., Scacco, S. C., Vergari, R., Solarino, G., Santacroce, G. and Papa, S. (1994). Decline with age of the respiratory chain activity in human skeletal muscle. *Biochim. Biophys. Acta* **1226**, 73-82.

Boyer, L. A., Plath, K., Zeitlinger, J., Brambrink, T., Medeiros, L. A., Lee, T. I., Levine, S. S., Wernig, M., Tajonar, A., Ray, M. K. et al. (2006). Polycomb complexes repress developmental regulators in murine embryonic stem cells. *Nature* **441**, 349-353.

Burighel, P. and Schiavinato, A. (1984). Degenerative regression of the digestive tract in the colonial ascidian *Botryllus schlosseri* (Pallas). *Cell Tissue Res.* **235**, 309-318.

Byrne, E., Trounce, I. and Dennett, X. (1991). Mitochondrial theory of senescence: respiratory chain protein studies in human skeletal muscle. *Mech. Ageing Dev.* **60**, 295-302.

Choi, J., Shendrik, I., Peacocke, M., Peehl, D., Buttyan, R., Ikeguchi, E. F., Katz, A. E. and Benson, M. C. (2000). Expression of senescence-associated beta-galactosidase in enlarged prostates from men with benign prostatic hyperplasia. *Urology* **56**, 160-166.

Cooper, J. M., Mann, V. M. and Schapira, A. H. V. (1992). Analyses of mitochondrial respiratory chain function and mitochondrial DNA deletion in human skeletal muscle: effect of ageing. *J. Neurol. Sci.* **113**, 91-98.

Eckert, R. L., Adhikary, G., Rorke, E. A., Chew, Y. C. and Balasubramanian, S. (2011). Polycomb group proteins are key regulators of keratinocyte function. *J. Invest. Dermatol.* **131**, 295-301.

Gilbert, S. F. (2000). *Developmental Biology*, 6th edition, pp. 749. Sunderland, MA: Sinauer Associates.

Hebert, S. L., Lanza, I. R. and Nair, K. S. (2010). Mitochondrial DNA alterations and reduced mitochondrial function in aging. *Mech. Ageing Dev.* **131**, 451-462.

Iakova, P., Awad, S. S. and Timchenko, N. A. (2003). Aging reduces proliferative capacities of liver by switching pathways of C/EBPalpha growth arrest. *Cell* **113**, 495-506.

Itahana, K., Campisi, J. and Dimri, G. P. (2007). Methods to detect biomarkers of cellular senescence: the senescence-associated beta-galactosidase assay. *Methods Mol. Biol.* **371**, 21-31.

Kaneko, N., Katsuyama, Y., Kawamura, K. and Fujiwara, S. (2010). Regeneration of the gut requires retinoic acid in the budding ascidian Polyandrocarpa misakiensis. *Dev. Growth Differ.* **52**, 457-468.

Kawamura, K. (1984). Morphogenetic tissue interactions during posterior commitment in palleal buds of the polystyelid ascidian, *Polyandrocarpa misakiensis*. *Dev. Biol.* **106**, 379-388.

Kawamura, K. and Fujiwara, S. (1994). Transdifferentiation of pigmented multipotent epithelium during morphallactic development of budding tunicates. *Int. J. Dev. Biol.* **38**, 369-377.

Kawamura, K. and Nakauchi, M. (1986). Mitosis and body patterning during morphallactic development of palleal buds in ascidians. *Dev. Biol.* **116**, 39-50.

Kawamura, K. and Sunanaga, T. (2010). Hemoblasts in colonial tunicates: are they stem cells or tissue-restricted progenitor cells? *Dev. Growth Differ.* **52**, 69-76.

Kawamura, K., Ookawa, S., Michibata, H. and Nakauchi, M. (1988). Autoradiographic studies on cell population kinetics in epithelial and haematopoietic stem cell lines in the process of palleal budding of asicidians. *Mem. Fac. Sci. Kochi Univ. Ser. D* **9**, 1-12.

Kawamura, K., Sugino, Y. M., Sunanaga, T. and Fujiwara, S. (2008a). Multipotent epithelial cells in the process of regeneration and asexual reproduction in colonial tunicates. *Dev. Growth Differ.* **50**, 1-11.

Kawamura, K., Tachibana, M. and Sunanaga, T. (2008b). Cell proliferation dynamics of somatic and germline tissues during zooidal life span in the colonial tunicate Botryllus primigenus. *Dev. Dyn.* **237**, 1812-1825.

Kawamura, K., Takakura, K., Mori, D., Ikeda, K., Nakamura, A. and Suzuki, T. (2012). Tunicate cytostatic factor TC14-3 induces a polycomb group gene and histone modification through Ca^{2+} binding and protein dimerization. *BMC Cell Biol.* **13**, 3.

Kelly, D. P. and Scarpulla, R. C. (2004). Transcriptional regulatory circuits controlling mitochondrial biogenesis and function. *Genes Dev.* **18**, 357-368.

Kirkwood, T. B. (2005). Time of our lives. What controls the length of life? *EMBO Rep.* **6**, Spec. No., S4-S8.

Konuma, T., Oguro, H. and Iwama, A. (2010). Role of the polycomb group proteins in hematopoietic stem cells. *Dev. Growth Differ.* **52**, 505-516.

Kuzmichev, A., Margueron, R., Vaquero, A., Preissner, T. S., Scher, M., Kirmizis, A., Ouyang, X., Brockdorff, N., Abate-Shen, C., Farnham, P. et al. (2005). Composition and histone substrates of polycomb repressive group complexes change during cellular differentiation. *Proc. Natl. Acad. Sci. USA* **102**, 1859-1864.

Lauzon, R. J., Patton, C. W. and Weissman, I. L. (1993). A morphological and immunohistochemical study of programmed cell death in *Botryllus schlosseri* (Tunicata, Ascidiacea). *Cell Tissue Res.* **272**, 115-127.

Lauzon, R. J., Rinkevich, B., Patton, C. W. and Weissman, I. L. (2000). A morphological study of nonrandom senescence in a colonial urochordate. *Biol. Bull.* **198**, 367-378.

Lee, B. Y., Han, J. A., Im, J. S., Morrone, A., Johung, K., Goodwin, E. C., Kleijer, W. J., DiMaio, D. and Hwang, E. S. (2006). Senescence-associated beta-galactosidase is lysosomal beta-galactosidase. *Aging Cell* **5**, 187-195.

Liu, L., Trimarchi, J. R. and Keefe, D. L. (2000). Involvement of mitochondria in oxidative stress-induced cell death in mouse zygotes. *Biol. Reprod.* **62**, 1745-1753.

Matsumoto, J., Nakamoto, C., Fujiwara, S., Yubisui, T. and Kawamura, K. (2001). A novel C-type lectin regulating cell growth, cell adhesion and cell differentiation in budding tunicates. *Development* **128**, 3339-3347.
Oda, T. and Watanabe, H. (1986). Developmental pattern of colonies in the polystyelid ascidian, Polyandrocarpa misakiensis. *Int. J. Invert. Repr. Dev.* **10**, 187-199.
Parkes, T. L., Elia, A. J., Dickinson, D., Hilliker, A. J., Phillips, J. P. and Boulianne, G. L. (1998). Extension of Drosophila lifespan by overexpression of human SOD1 in motorneurons. *Nat. Genet.* **19**, 171-174.
Rajasekhar, V. K. and Begemann, M. (2007). Concise review: roles of polycomb group proteins in development and disease: a stem cell perspective. *Stem Cells* **25**, 2498-2510.
Scarpulla, R. C. (2008). Transcriptional paradigms in mammalian mitochondrial biogenesis and function. *Physiol. Rev.* **88**, 611-638.
Sunanaga, T., Watanabe, A. and Kawamura, K. (2007). Involvement of vasa homolog in germline recruitment from coelomic stem cells in budding tunicates. *Dev. Genes Evol.* **217**, 1-11.
Timchenko, N. A. (2009). Aging and liver regeneration. *Trends Endocrinol. Metab.* **20**, 171-176.
Tiozzo, S., Ballarin, L., Burighel, P. and Zaniolo, G. (2006). Programmed cell death in vegetative development: apoptosis during the colonial life cycle of the ascidian Botryllus schlosseri. *Tissue Cell* **38**, 193-201.
Watanabe, H. and Tokioka, T. (1972). Two new species and one possibly new race of social styelids from Sagami Bay, with remarks on their life history, especially the mode of budding. *Publ. Seto Mar. Biol. Lab.* **14**, 327-345.
Yang, H. and Fogo, A. B. (2010). Cell senescence in the aging kidney. *J. Am. Soc. Nephrol.* **21**, 1436-1439.
Zamboni, L. and DeMartino, C. (1967). Buffered picric acid-formaldehyde: A new, rapid fixative for electron microscopy. *J. Cell Biol.* **35**, 148A.

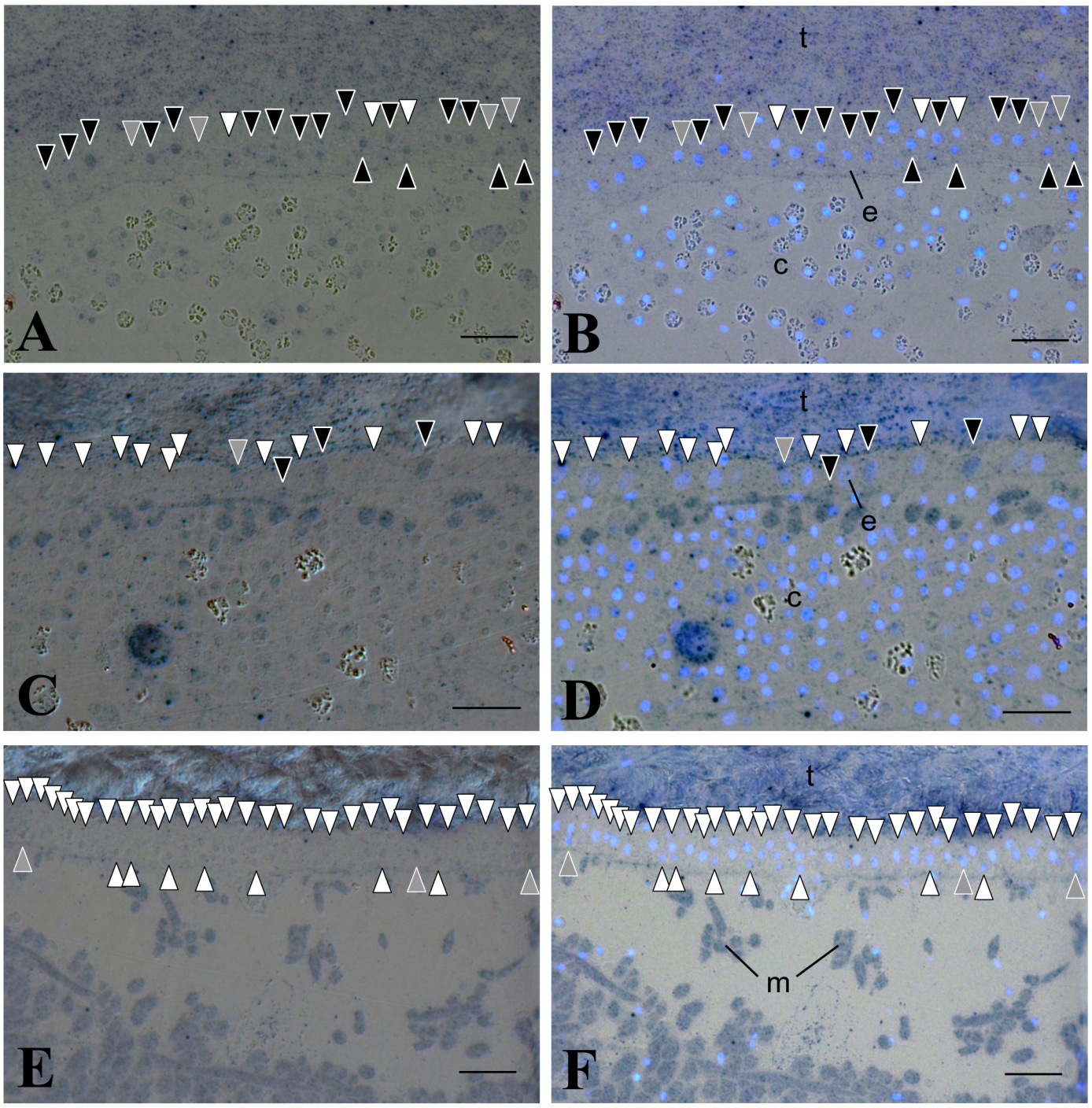

Fig. S1. PCNA expression in epidermal nuclei during budding and zooid senescence. (**A**,**B**) Growing bud. (**C**,**D**) Juvenile zooid. (**E**,**F**) Senescent adult zooid. (A,C,E) Anti-PCNA immunostaining. (B,D,F) Immunostaining merged with DAPI staining. Black and grey arrowheads show strong and moderate PCNA expression, respectively. White arrowheads show no PCNA staining. c, coelomic cell; e, epidermis; m, body muscle cell; t, tunic. Scale bars: 20 µm.

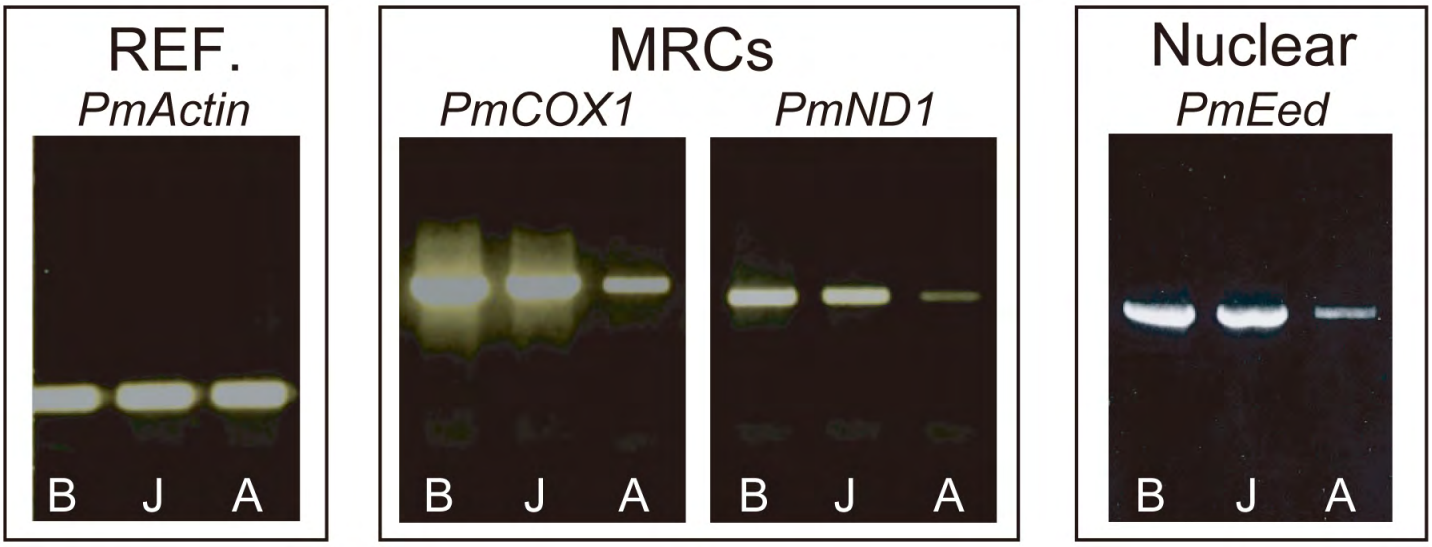

Fig. S2. RT-PCR analysis of the expression of *Polyandrocarpa* MRCs, *PmCOX1* and *PmND1*, and nuclear gene *PmEed* at different ageing stages. mRNAs were extracted from growing buds (B), juvenile zooids (J) and senescent adult zooids (A). Cytoplasmic actin was used as internal standard.

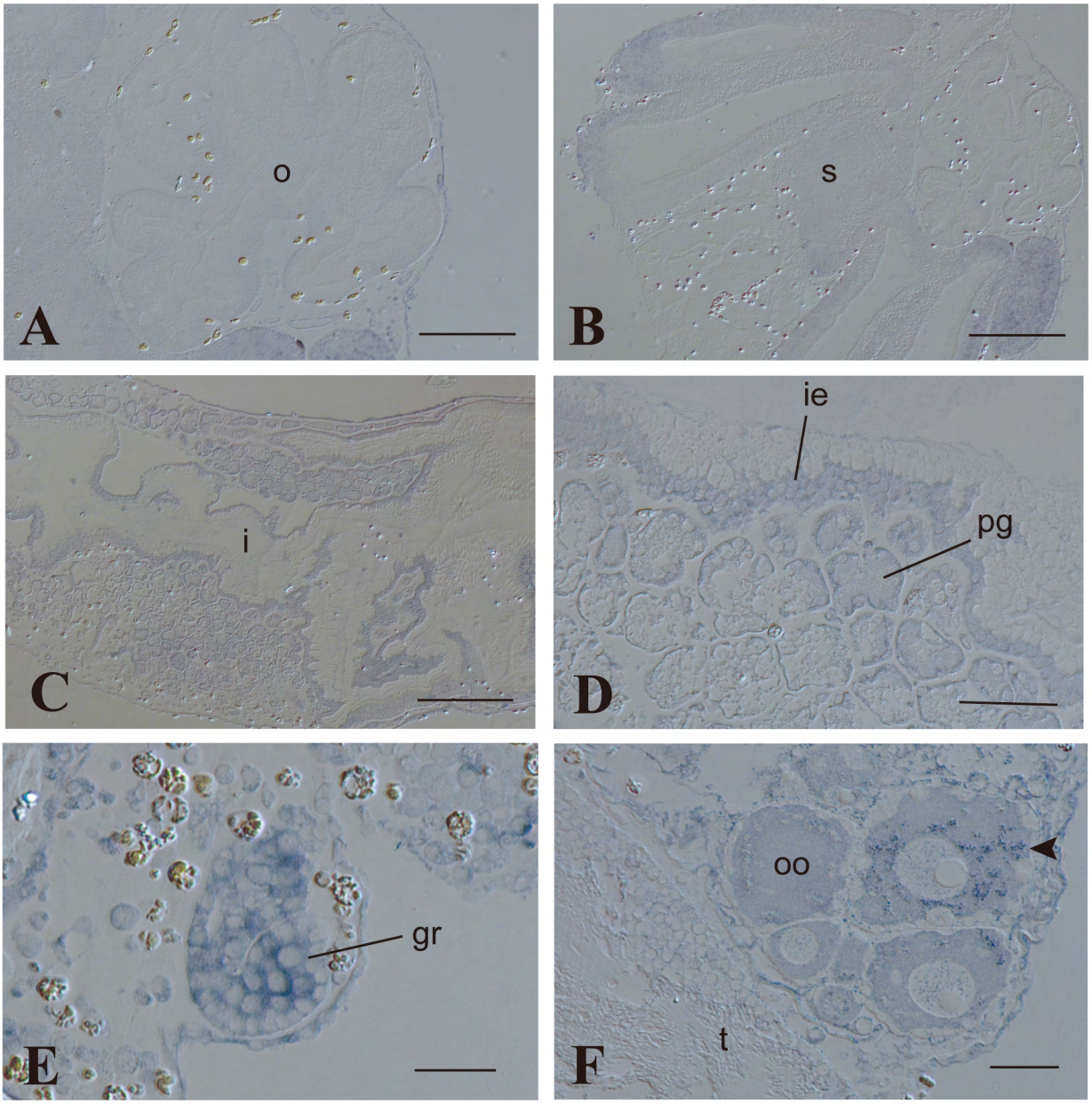

Fig. S3. Expression of *PmCOX1* in differentiated tissues; in situ hybridization. (**A**) Oesophagus. Scale bar: 50 μm. (**B**) Stomach. Scale bar: 50 μm. (**C**) Intestine. Scale bar: 100 μm. (**D**) Higher magnification of (C). Scale bar: 25 μm. (**E**) Gonad rudiment. Scale bar: 20 μm. (**F**) Ovary. Arrowhead shows an aggregate of dotted signals probably from mitochondria. Scale bar: 20 μm. gr, gonad rudiment; i, intestine; ie, intestinal epithelium; o, oesophagus; oo, oocyte; pg, pyloric gland; s, stomach; t, testis.

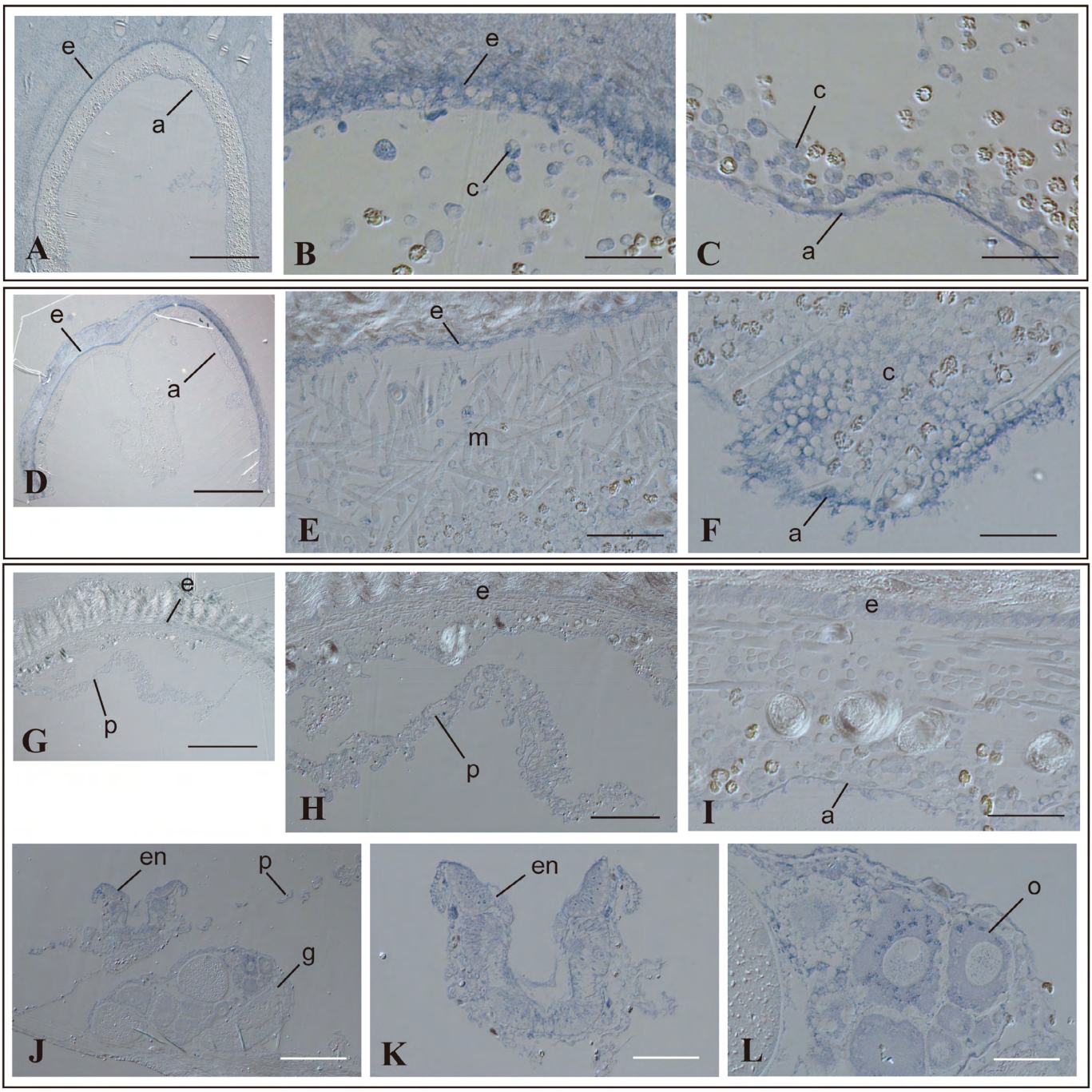

Fig. S4. *PmND1* expression at different ageing stages; in situ hybridization. (**A-C**) Growing buds. (A) Lower magnification. Scale bar: 200 µm. (B) Epidermis and coelomic cells. Scale bars: 20 µm. (C) Atrial epithelium and coelomic cells. Scale bar: 20 µm. (**D-F**) Juvenile zooids. (D) Lower magnification. Scale bar: 300 µm. (E) Epidermis and body muscle tissue. Scale bar: 30 µm. (F) Atrial epithelium and coelomic cells. Scale bar: 20 µm. (**G-L**) Senescent zooids. (G) Lower magnification. Scale bar: 300 µm. (H) Body wall and pharynx. Scale bar: 100 µm. (I) Epidermis, coelomic cells and atrial epithelium. Scale bar: 20 µm. (J) Ventral organs. Scale bar: 100 µm. (K) Endostyle. Scale bar: 50 µm. (L) Gonad. Scale bar: 50 µm. a, atrial epithelium; c, coelomic cell, e, epidermis; en, endostyle; g, gonad; m, body muscle cell; o, oocyte; p, pharynx.

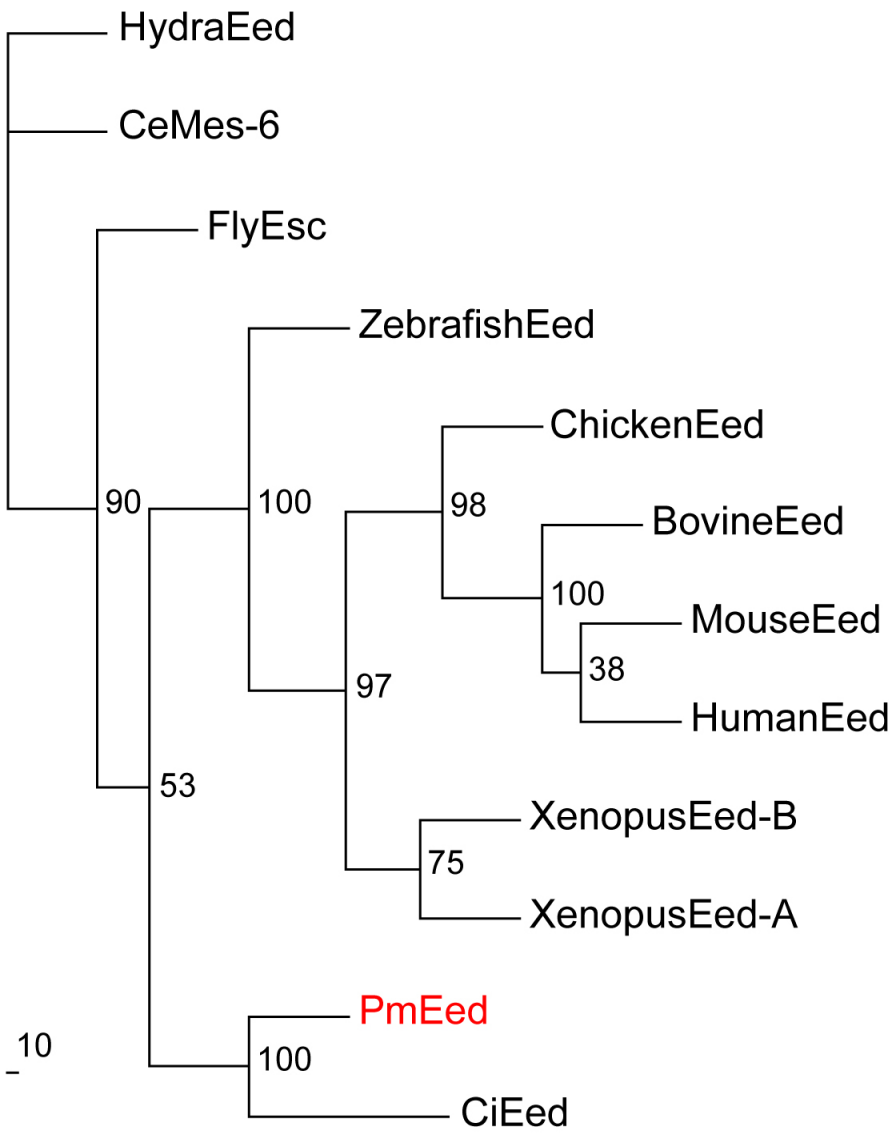

Fig. S5. Molecular phylogeny of the nuclear gene *PmEed*. Phylogenetic relationship among partial amino acid sequence of Eed proteins is shown. The analysis was carried out with the maximum likelihood method. The bootstrap values are shown on each branch. Ce, *Caenohabditis elegans*; Ci, *Ciona intestinalis*; Pm, *Polyandrocarpa misakiensis*.

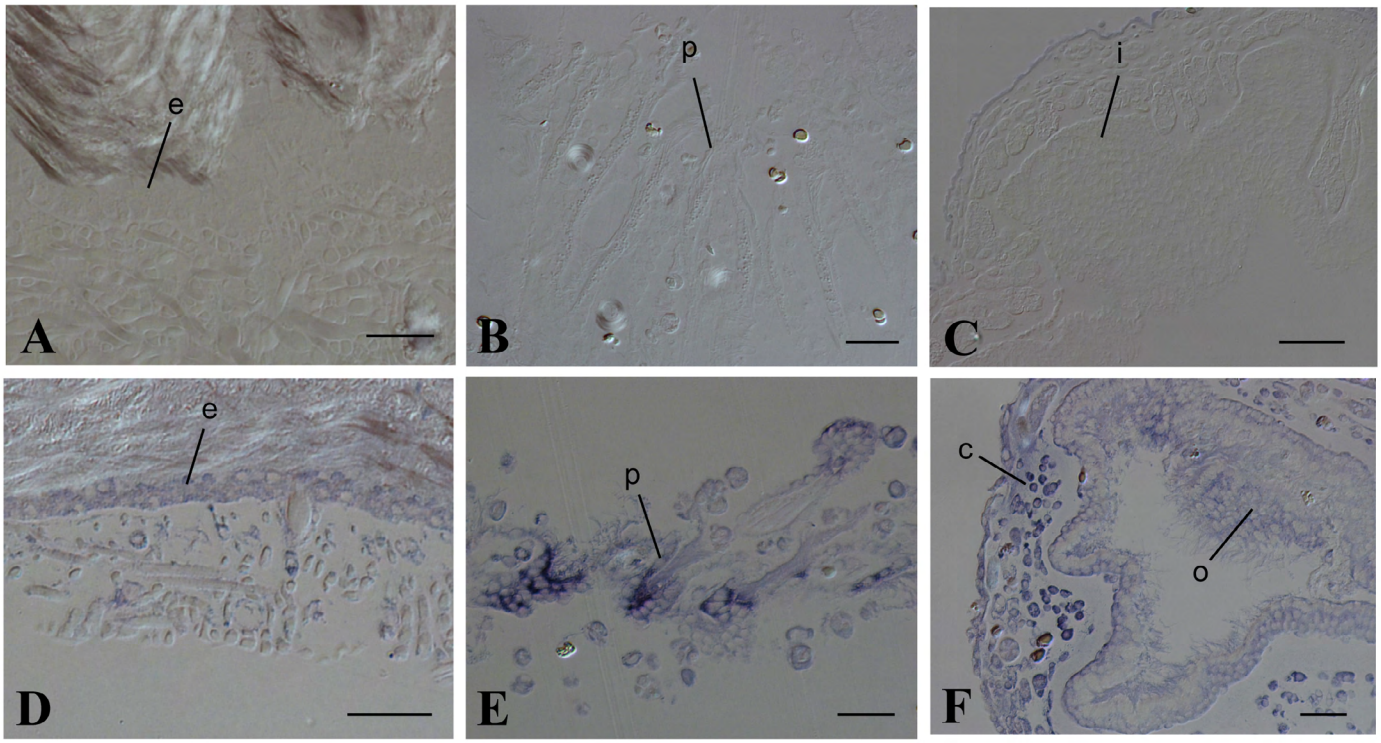

Fig. S6. Effect of TC14-3 on *PmEed* expression in senescent zooid pieces; in situ hybridization. (**A-C**) Negative control. Senescent zooids were only cut into pieces. (A) Epidermis. Scale bars: 20 μm. (B) Pharynx. Scale bars: 20 μm. (C) Digestive tract. Scale bars: 40 μm. (**D-F**) TC14-3-treated zooid pieces. (D) Epidermis and coelomic cells. Scale bars: 20 μm. (E) Pharynx. Scale bars: 20 μm. (F) Digestive tract and coelomic cells. Scale bars: 20 μm. c, coelomic cell; e, epidermis; i, intestine; o, oesophagus; p, pharyngeal epithelium.

Table S1. Number of epidermal mitochondria during senescence

Stage	Number of mitochondria/20 μm^2
Growing bud	8.9±1.4*
Juvenile zooids	6.9±1.9
Senescent zooids	6.2±2.0

*Average±s.d.